BioMACROMOLECULES

Article

Design of polysaccharide-b-elastin like polypeptide bioconjugates and their thermoresponsive self-assembly

Ye Xiao, Zoeisha S. Chinoy, Gilles Pecastaings, Katell Bathany, Elisabeth Garanger, and Sebastien Lecommandoux

Just Accepted

Design of polysaccharide-*b*-elastin like polypeptide bioconjugates and their thermoresponsive self-assembly

Ye Xiao,[†§] Zoeisha S. Chinoy,[†§] Gilles Pecastaings,[†] Katell Bathany,[‡] Elisabeth Garanger,[†] and*

Sébastien Lecommandoux[†]*

† Univ. Bordeaux, CNRS, Bordeaux INP, LCPO, UMR 5629, F-33600, Pessac, France

‡ Univ. Bordeaux, CNRS, Bordeaux INP, Chimie et Biologie des Membranes et des Nano-objets

(UMR 5248), Allée Geoffroy Saint Hilaire, F-33600, Pessac, France

§ Authors contributed equally to this work

1

ABSTRACT

The advantageous biological properties of polysaccharides and precise stimuli-responsiveness of elastin-like polypeptides (ELPs) are of great interest for the design of polysaccharide and polypeptide-based amphiphilic block copolymers for biomedical applications. Herein, we report the synthesis and characterization of a series of polysaccharide-*block*-ELP copolymers, containing two biocompatible and biodegradable blocks coupled *via* copper(I)-catalyzed azide-alkyne cycloaddition (CuAAC). The resulting bioconjugates are capable of self-assembling into well-defined nanoparticles in aqueous solution upon raising the solution temperature above a specific transition temperature (T_t) – a characteristic of the ELP moiety. To the best of our knowledge, this is the first study where polysaccharides were combined with a stimuli-responsive ELP for the preparation of thermo-sensitive self-assemblies, providing insight into novel pathways for designing bioinspired stimuli-responsive self-assemblies for biomedical applications.

INTRODUCTION

Nanostructured carriers resulting from the self-assembly of amphiphilic block copolymers have been developed for a broad range of applications, ranging from biomimetics[1-3] to nanomedicines.[4,5] Numerous synthetic polymers have been selected as building blocks due to their biocompatibility and low cytotoxicity, such as poly(ethylene glycol),[6,7] poly(L-glutamic acid),[8,9] poly(γ-benzyl-L-glutamate),[10-12] poly(2-hydroxyethyl methacrylate),[13,14] polylactide,[15,16] polycaprolactone,[17] and poly(trimethylene carbonate),[9,18] and have been approved for biomedical applications by regulatory agencies. Additionally, biologically derived or inspired polymers, like polysaccharides[19-21] and polypeptides[22], show considerable promise as block copolymer

constructs since they are naturally biodegradable, biocompatible and are potentially

biofunctional. Regarding the biomedical application of block copolymers as carriers, a key

challenge is to enhance accumulation of the active components at the biological target.[23] A

typical method to achieve this goal is to introduce bioactive targeting moieties on the surface of

nano-objects.[24-26] Such surface decorated strategies have led to the design of original bioactive

block copolymers that favor the use of natural targeting functionalities.[27-29] In this respect,

bioactive polysaccharides-based (*e.g.,* chitosan,[30,31] galactan,[32] fucoidan,[33] hyaluronan[11,34]) block

copolymers able to recognize and bind to specific receptors demonstrate particularly promising

interest for potential biomedical applications.[35]

Recently, stimuli-responsive polymer nanosystems[36-41] have been extensively explored due to

their ability of supramolecular assembly or disassembly in response to "internal stimuli", such as

pH,[42,43] reductive-oxidative environment[44,45] and enzymes,[46] or "external stimuli", such as

temperature,[47,48] light[49,50] and magnetic field[51]. Among them, recombinant elastin-like

polypeptides (ELPs) have gained significant attention as stimuli-responsive protein-like

polymers.[52-54] In aqueous solution, ELPs display a lower critical solution temperature (LCST),

similar to synthetic thermo-responsive polymers such as poly(*N*-isopropyl acrylamide)

PNIPAM,[55] also referred to as inverse transition temperature (T_t) that actually corresponds to the

cloud point temperature. Below the T_t, ELPs are water soluble, while upon heating the solution

temperature above the T_t, ELPs aggregate into insoluble coacervates, this phase transition being

fully reversible. T_t can be highly tunable either by playing with molecular parameters such as

varying amino acid residues composition and protein molecular weight, or by controlling

environmental parameters such as concentration, pH or cosolutes.[56-58] Post-translational chemical

modification of ELPs, for example, chemoselective modifications of ELPs at the *C*- or *N*-

terminal end,[59] or at specific residues such as methionine,[60-62] cysteine,[63,64] tyrosine,[65] or lysine,[66,67] has also been exploited for tuning the T_t of specific ELPs, as well as for facilitating subsequent conjugation of ELPs with polymers,[59,66] dyes,[64] or drugs[67,68]. ELP diblock copolymers could be obtained by fusing ELP blocks with different T_t, which self-assembled into micelles by triggering the phase transition of the ELP block with the lowest T_t.[69-72] The stimuli-responsive property of ELPs has also been exploited to obtain well-defined ELP-based nanomedicines, such as ELP-proteins,[73] ELP-drug conjugates,[67] and ELP-nucleic acid complexes.[74] Moreover, as a building block of copolymers, combinations of ELPs with other types of polymer-based blocks, such as poly(γ-benzyl-L-glutamate),[75] poly(L-glutamic acid),[8] poly(aspartic acid),[76] poly(ethylene glycol),[59,77] and polyelectrolyte[78] has demonstrated to be a fascinating strategy to obtain functional block copolymers which could self-assemble in aqueous conditions above a specific and tunable T_t.

Although polysaccharides and polypeptides-based block copolymers were reported for decades, benefits from conjugates of polysaccharides with ELPs have not yet been investigated, since a highly efficient and proper conjugation method is required. We previously synthesized polysaccharide-*b*-polypeptide block copolymers *via* copper(I)-catalyzed azide-alkyne cycloaddition (CuAAC) for the preparation of glycoprotein biomimetic vesicles,[11,12] and demonstrated the interest of such design as drug-delivery nanocarriers.[79,80] To be able to use CuAAC "click" chemistry for conjugation, polysaccharides and ELPs need to be functionalized with either an azide or an alkyne group.[81] Polysaccharides can be readily modified at the reducing end with azide-containing linkers using reductive amination,[11,12] or by using bifunctional oxyamine, oxime or *N*-methoxyamine linkers[82,83]. Regarding the introduction of an alkyne group at the ELP chain end, an alkyne functionalized *N*-hydroxysuccinimide ester (NHS-

ester) can be easily prepared and coupled with the *N*-terminal primary amine group, granting the ELP with a functional moiety to conjugate with the polysaccharide.[84]

We present here, a modular approach that combines polysaccharide and ELP into block copolymers capable of self-assembling into nanoparticles in aqueous solution upon heating above a specific T_t. Both block being composed of biological molecules, make the polysaccharide-*b*-ELP bioconjugates biocompatible, biodegradable and possibly bioactive. The versatile choice of polysaccharide and ELP allow "tailor-made" design of bioconjugates for a desired propose, such as specific receptor binding and drug loading. The ELP block can be further modified at methionine residues, allowing subsequent orthogonal biofunctionalization of bioconjugates with small molecules such as dyes or inter-chain cross-linking. Three different polysaccharides namely dextran,[10,12] laminarihexaose[85,86] and hyaluronic acid,[11,25,34] were functionalized with an azide moiety at their reducing end, while the ELP was modified with an alkyne moiety at the *N*-terminus by NHS-coupling chemistry. Three polysaccharide-*b*-ELP bioconjugates were thus prepared through click chemistry, isolated and subsequently fully characterized. Their transition temperature behaviors were studied through turbidity measurements by ultraviolet–visible (UV-Vis) spectroscopy and their self-assembly properties were subsequently investigated by temperature-varying dynamic light scattering (DLS) and temperature-controlled liquid atomic force microscopy (Liquid AFM). To our knowledge, the synthesis and temperature-triggered self-assembly behavior study of polysaccharide-*b*-ELPs block copolymers were demonstrated for the first time, providing insight

into original pathways for designing bioactive thermo-sensitive self-assemblies for biomedical applications.

EXPERIMENTAL SECTION

Materials

Acrolein (95%), sodium azide (NaN$_3$, 99.5%), acetic acid (AcOH, 99.8%), methoxylamine hydrochloride (98%), sodium cyanoborohydride (NaBH$_3$CN, 95%), hydrochloric acid (HCl, 37%), 4-pentynoic acid (97%), *N,N'*-dicyclohexylcarbodiimide (DCC, 99%), *N*-hydroxysuccinimide (NHS, 98%), trimethylamine (TEA, 99%), copper(II) sulfate pentahydrate (CuSO$_4$, 99%), dichloromethane (DCM, 99.9%), *N,N*-dimethylformamide (DMF, 99.8%), dimethyl sulfoxide (DMSO, 99.7%), methanol (MeOH, 99.8%), diethyl ether (99.9%) and anhydrous magnesium sulfate (MgSO$_4$, 99.5%) were purchased from Sigma-Aldrich. *N,N*-Diisopropylethylamine (DIPEA, 99%), sodium acetate (AcONa, 99%) and sodium ascorbate (NaAsc, 99%) were obtained from Alfa Aesar. Tris(benzyltriazolylmethyl)amine (TBTA, 97%) were purchased from TCI. Cuprisorb® was purchased from Seachem. Dextran (Dex, T10) was purchased from pharmacosmos. Laminarihexaose (Lam) was purchased from Megazyme. Sodium hyaluronate (HA) was purchased from Lifecore Biomedical. Water was purified using an ELGA PURELAB Classic system. Solvent was purified using PureSolv MD-5 solvent purification system from Innovative Technology. Dialysis was conducted using a Spectra/Por®6 dialysis membrane.

Synthetic Procedure

Synthesis of N-(3-azidopropyl)-O-methylhydroxylamine (Azide-linker, 1). Acrolein (1.84 mL, 27.4 mmol) was added to acetic acid (4 mL) at -20 °C, followed by dropwise addition of a solution of sodium azide (2.38 g, 41.2 mmol) in H_2O (10.4 mL). The reaction mixture was let to stir at -20 °C for 1.5 hour. It was then quenched with a saturated solution of $NaHCO_3$ (80 mL) and the resulting mixture was extracted with DCM (2 × 100 mL). The combined organic extracts were washed with sat. aq. $NaHCO_3$ (150 mL), dried over $MgSO_4$, filtered and concentrated *in vacuo* to 100 mL. To the solution in DCM, methoxylamine hydrochloride (2.68 g, 31.68 mmol) and sodium acetate (4.42 g, 54 mmol) were added and the mixture was stirred overnight at r.t. Sat. aq. $NaHCO_3$ (150 mL) was added to quench the reaction and the resulting mixture was then extracted with DCM (2 × 100 mL). The combined organic extracts were washed with Sat. aq. $NaHCO_3$ (150 mL), dried over $MgSO_4$, filtered and concentrated *in vacuo* to 100 mL. To the solution in DCM, $NaBH_3CN$ (2 g, 32 mmol) was added, followed by dropwise addition of 1M ethanolic HCl (32 mL, freshly prepared by adding acetyl chloride to ethanol). The reaction mixture was stirred at r.t for 1.5 hour, concentrated and the resulting white solid suspended in sat. aq. $NaHCO_3$ (150 mL) and extracted with DCM (2 × 100 mL). The combined organic extracts were washed with sat. aq. $NaHCO_3$ (150 mL), dried over $MgSO_4$, filtered and concentrated *in vacuo* to afford the crude *N*-(3-azidopropyl)-*O*-methylhydroxylamine as a yellow oil. Purification of the crude product by silica gel column chromatography (1-3% MeOH in DCM) yielded *N*-(3-azidopropyl)-*O*-methylhydroxylamine as a colorless oil (Azide-linker, 2.2 g, 62% over 3 steps). ^{1}H NMR (400 MHz, $CDCl_3$): δ 3.55 (s, 3H, C*H*$_3$O), 3.41 (t, 2H, C*H*$_2$N$_3$), 3.00 (t, 2H, NHC*H*$_2$), 1.83 (p, 2H, CH$_2$C*H*$_2$CH$_2$). ^{13}C NMR (101 MHz, $CDCl_3$): δ 62.01 (*C*H$_3$O), 49.44 (*C*H$_2$N$_3$), 48.94 (NH*C*H$_2$), 26.87 (CH$_2$*C*H$_2$CH$_2$). In agreement with the literature data.[82]

Synthesis of Dextran-Azide (Dex-N₃, 2). The azide-linker (380 mg, 2.9 mmol) was added to a solution of dextran (MW=8,000 Da, 1 g, 125 µmol) in acetate buffer (AcOH / AcONa, 2 M, pH 4.6, 4.2 mL), and the reaction mixture was incubated at 40 °C with shaking, for 9 days. The product was purified by dialysis (dialysis bag MWCO 1 kDa) against pure water for 24 hour (changing water 3 times per day), followed by lyophilization to obtain the product as a white powder (805 mg, 79% yield). ^{1}H NMR (400 MHz, D_2O): δ 4.98 (d, H-1), 4.18 (d, C*H*N(OCH₃)CH₂), 4.04-3.97 (m, H-6), 3.95–3.89 (m, H-5), 3.69–3.80 (br m, H-6', H-3), 3.61–3.37 (br m, H-2, H-4, C*H₂*N₃), 3.20–3.13 (dt, CHN(OCH₃)C*H₂*), 3.01–2.93 (dt, CHN(OCH₃)C*H₂'*), 1.92–1.88 (m, CH₂C*H₂*CH₂). FT-IR (ATR): 3368, 2906, 2106 (υ_{azide}), 1351, 1148, 1164, 1007, 915, 846, 763, 545, 429 cm^{-1}.

Synthesis of Laminarihexaose-Azide (Lam-N₃, 3). The azide-linker (900 mg, 6.9 mmol) was added to a solution of laminarihexaose (500 mg, 0.5 mmol) in acetate buffer (AcOH / AcONa, 2 M, pH 4.6, 5 mL), and the reaction mixture incubated at 40 °C with shaking, for 8 days (vortexing 3 times per day). Then the mixture was lyophilized and re-dissolved in water 5 mL, purified by dialysis (dialysis bag MWCO 100 Da) against pure water for 3 days (changing water 3 times per day and transferring excess dialysis solution to new dialysis bag every 12 hour), followed by lyophilization to obtain the product as a white powder (302 mg, 54% yield). ^{1}H NMR (400 MHz, D_2O): δ 4.81 (d, H-1), 4.23 (m, C*H*N(OCH₃)CH₂), 3.97–3.88 (m, H-6), 3.86–3.68 (br m, H-6',H-3), 3.67–3.33 (br m, H-2,H-4,H-5, C*H₂*N₃), 3.22–3.13 (m, CHN(OCH₃)C*H₂'*), 3.03–2.95 (m, CHN(OCH₃)C*H₂*), 1.91 (m, CH₂C*H₂*CH₂). FT-IR (ATR): 3434, 3151, 2890, 2100 (υ_{azide}), 1568, 1403, 1308, 1159, 1072, 1022, 896, 557 cm^{-1}.

Synthesis of Hyaluronan-Azide (HA-N₃, 4). The azide-linker (520 mg, 4 mmol) and sodium cyanoborohydride (65 mg, 1 mmol) were added to a solution of sodium hyaluronate (MW=

7,000 Da, 1 g, 0.14 mmol) in acetate buffer (AcOH / AcONa, 2 M, pH 5.5, 5 mL), and the reaction mixture was incubated at 50 °C with shaking, for 5 days. The product was purified by dialysis (dialysis bag MWCO 1 kDa) against pure water for 24 hour (changing water 3 times per day), followed by lyophilization to obtain the product as a white powder. (610 mg, 60% yield). ^{1}H NMR (400 MHz, D$_2$O): δ 4.56 (d, GlcNAc H-1), 4.48 (d, GlcUA H-1), 3.99–3.67 (br m, GlcNAc H-6, H-2, H-3, H-5, GlcUA H-4), 3.66–3.41 (br m, GlcNAc H-4, GlcUA H-3, H-5, CH_2N$_3$), 3.35 (t, GlcUA H-2), 2.94–2.86 (m, CH$_2$N(OCH$_3$)CH_2), 2.03 (s, GlcNAc COCH$_3$), 1.87 (m, CH$_2$CH_2CH$_2$). FT-IR (ATR): 3323, 2892, 2107 (υ$_{azide}$), 1729, 1642, 1555, 1376, 1315, 1152, 1042, 610 cm^{-1}.

Synthesis of 4-Pentynoic Acid Succinimidyl Ester (Pentynoic NHS-ester, 5). *N, N'*-dicyclohexylcarbodiimide (480 mg, 2.3 mmol) was added to a solution of pentynoic acid (210 mg, 2.14 mmol) in DCM (8mL) and the mixture was stirred at r.t for 5 min and then N-hydroxysuccinimide (260 mg, 2.3 mmol) was added. The reaction was continuously stirred at r.t for 3 hour more. Afterwards, the precipitated dicyclohexylurea was filtered over Celite and washed with cold DCM (2×10mL). The filtrate was collected and DCM was removed *in vacuo*. The crude product was re-dissolved in EtOAc (10 mL) and cooled in a refrigerator at 0 °C for 20 min. The precipitate was filtered over Celite, and the filtrate was washed with saturated NaHCO$_3$ (2×50 mL) and brine (2×50 mL), dried over MgSO$_4$, filtered and concentrated *in vacuo* to give the crude product as a colorless oil. Purification of the oil by silica gel column chromatography (petroleum ether/EtOAc = 2:1) yielded pentynoic NHS-ester as a white solid (300 mg, 72% yield). ^{1}H NMR (400 MHz, CDCl$_3$): δ 2.90–2.82 (m, 6H, COCH_2CH$_2$CO, OCOCH_2CH$_2$), 2.62 (ddd, 2H, CH_2C≡CH), 2.05 (t, 1H, C≡CH). ^{13}C NMR (101 MHz, CDCl$_3$): δ 168.89

(COCH$_2$CH$_2$CO), 167.02 (OCOCH$_2$), 80.84 (CH$_2$$C$≡CH), 70.04 (CH$_2$C≡$C$H), 30.31 (OCO$C$H2),

25.57 (COCH$_2$$CH_2$CO), 14.09 ($CH_2$C≡CH).

Synthesis of ELP-Alkyne (ELP-Alk, 6). Pentynoic NHS-ester (92 mg, 0.47 mmol) and *N,N*-diisopropylethylamine (1.7 mg, 13.2 µmol) were added to a solution of ELP (MW= 17,035 Da, 225 mg, 13.2 µmol) in anhydrous DMSO (18 mL) and the mixture was stirred at r.t for 72h. It was then diluted with pure water (20 mL). The product was purified by dialysis (dialysis bag MWCO 15 kDa) against pure water for 48 h (changing water 3 times per day), followed by lyophilization to obtain the ELP-Alk as a white powder (210 mg, 93% yield). ^{1}H NMR (400 MHz, D$_2$O): δ 7.63–7.09 (br, indole *H* Trp), 4.57 (m, CH_α Met), 4.45 (m, CH_α Val, Pro), 4.19 (d, CH_α Val$_{Xaa}$), 4.06–3.89 (br m, C$H_{2\alpha}$ Gly, C$H_{2\delta}$ Pro), 3.75 (m, C$H_{2'\delta}$ Pro), 2.69–2.46 (br m, C$H_{2\gamma}$ Met, CH_2CH$_2$C≡CH), 2.33 (m, C$H_{2\beta}$ Pro), 2.18–1.91 (m, C$H_{2\beta}$ Met, C$H_{2'\beta}$ Pro, C$H_{2\gamma}$ Pro, CH_β Val, C$H_{3\epsilon}$ Met, CH$_2$C≡CH), 1.05–0.91 (m, C$H_{3\gamma}$ Val). MALDI-TOF: Calculated Mass = 17,115 Da, Experimental Mass [M+H]$^+$ = 17,120.5 Da.

Synthesis of Dextran-b-ELP (Dex-b-ELP, 7). Copper sulfate (6 mg, 22.8 µmol), sodium ascorbate (10 mg, 45.6 µmol) and TBTA (12 mg, 22.8 µmol) were added to a solution of ELP-Alk (65 mg, 3.8 µmol) and Dex-N$_3$ (46 mg, 5.7 µmol) in anhydrous DMSO (8 mL) under argon atmosphere and the reaction mixture was stirred at r.t for 3 days. It was then diluted with cold water (20 mL) and cooled in a refrigerator at 4 °C for 20 min. TBTA was precipitated and removed by centrifugation. Cuprisorb (120 mg) was added to the resulting solution and it was then incubated at r.t with shaking, for 18 h to remove the copper. The solution containing cuprisorb was centrifuged and the supernatant was purified by dialysis (dialysis bag 15 kDa) against pure water for 5 days (changing water 3 times per day), followed by lyophilization to obtain the product as a white powder (92 mg, 90 % yield). ^{1}H NMR (400 MHz, D$_2$O): δ 7.75 (s,

triazole H), 7.63–7.09 (br, indole H Trp), 4.99 (d, Dex H-1), 4.55 (m, $CH_α$ Met), 4.44 (m, $CH_α$ Val, Pro), 4.17 (d, $CH_α$ Val$_{Xaa}$), 4.06–3.87 (br m, $CH_{2α}$ Gly, $CH_{2δ}$ Pro, Dex H-6,H-5), 3.82-3.67 (m, $CH_{2'δ}$ Pro, Dex H-6',H-3), 3.62–3.49 (Dex H-2,H-4), 2.69–2.48 (br m, $CH_{2γ}$ Met), 2.31 (m, $CH_{2β}$ Pro), 2.18–1.89 (m, $CH_{2β}$ Met, $CH_{2'β}$ Pro, $CH_{2γ}$ Pro, $CH_β$ Val, $CH_{3ε}$ Met), 1.03–0.88 (m, $CH_{3γ}$ Val). FT-IR (ATR): 3332, 2929, 1653, 1527, 1443, 1342, 1152, 1106, 1017, 917, 547 cm^{-1}.

Synthesis of Laminarihexaose-b-ELP (Lam-b-ELP, 8). Copper sulfate (5.5 mg, 22 μmol), sodium ascorbate (9 mg, 45.4 μmol) were added to a solution of ELP-Alk (62 mg, 3.6 μmol) and Lam-N$_3$ (20 mg, 18.1 μmol) in anhydrous DMSO (8mL) under argon atmosphere and the reaction mixture was stirred at r.t for 3 days. It was then diluted with cold water (20 mL), after which Cuprisorb (110 mg) was added and the resulted solution was incubated at r.t with shaking, for overnight to remove the copper. The solution containing cuprisorb was centrifuged and the supernatant was purified by dialysis (dialysis bag MWCO 15 kDa) against pure water for 5 days (changing water 3 times per day), followed by lyophilization to obtain the product as a white powder (60 mg, 93% yield). ^{1}H NMR (400 MHz, D$_2$O): δ 7.74 (s, triazole H), 7.60–7.09 (br, indole H Trp), 4.80 (m, Lam H-1), 4.55 (m, $CH_α$ Met), 4.43 (m, $CH_α$ Val, Pro), 4.17 (d, $CH_α$ Val$_{Xaa}$), 4.05–3.85 (br m, $CH_{2α}$ Gly, $CH_{2δ}$ Pro, Lam H-6), 3.82-3.66 (m, $CH_{2'δ}$ Pro, Lam H-6',H-3), 3.62–3.34 (Lam H-2,H-4, H-5), 2.69–2.48 (br m, $CH_{2γ}$ Met), 2.41–2.24 (m, $CH_{2β}$ Pro), 2.19–1.88 (m, $CH_{2β}$ Met, $CH_{2'β}$ Pro, $CH_{2γ}$ Pro, $CH_β$ Val, $CH_{3ε}$ Met), 1.05–0.85 (m, $CH_{3γ}$ Val). FT-IR (ATR): 3322, 2917, 1654, 1522, 1440, 1221, 1105, 1063, 1027, 562 cm^{-1}.

Synthesis of Hyaluronan-b-ELP (HA-b-ELP, 9). HA-N$_3$ was first acidified by adding aq. HCl, so as to be totally soluble in DMSO. HA-N$_3$ (18mg, 3.5 μmol), copper sulfate (9 mg, 36 μmol), sodium ascorbate (18 mg, 90 μmol) and TBTA (22 mg, 41 μmol) were added to a solution of ELP-Alk (60 mg, 3.5 μmol) in anhydrous DMSO (6 mL) under argon atmosphere. The mixture

was stirred at 40 °C for 4 days, after which the reaction was diluted with cold water (20 mL) and cooled in a refrigerator at 4 °C for 20 min. TBTA was precipitated and removed by centrifugation. Cuprisorb (180 mg) was added to the resulted solution and it was then incubated at r.t with shaking, for overnight to remove the copper. The solution containing cuprisorb was centrifuged and the supernatant was purified by dialysis (dialysis bag MWCO 15 kDa) against pure water for 5 days (changing water 3 times per day), followed by lyophilization to obtain the crude product (53 mg). The crude product was redissolved in deionized water (5.3 mL) and the solution was then heated to 40 °C and kept for 1 h. The insoluble unreacted ELPs were centrifuged at 13,000 g for 20 min at 40 °C. The supernatant was lyophilized to give the final product as a white powder (42 mg, 54 % yield). ^{1}H NMR (400 MHz, D$_2$O): δ 7.75 (s, triazole H), 7.60–7.09 (br, indole H Trp), 4.62–4.37 (br, CH_α Met, Val, Pro, GlcUA H-1, GlcNAc H-1), 4.17 (d, CH_α Val$_{Xaa}$), 4.04–3.66 (br, C$H_{2\alpha}$ Gly, C$H_{2\delta}$ Pro, C$H_{2'\delta}$ Pro, GlcUA H-4, GlcNAc H-2, H-3, H-5, H-6), 3.65–3.42 (GlcUA H-3, H-5), 3.41–3.30 (t, GlcUA H-2), 2.69–2.48 (br m, C$H_{2\gamma}$ Met), 2.41–2.25 (m, C$H_{2\beta}$ Pro), 2.20–1.89 (m, C$H_{2\beta}$ Met, C$H_{2'\beta}$ Pro C$H_{2\gamma}$ Pro, CH_β Val, C$H_{3\epsilon}$ Met, CH_3 GlcNAc), 1.06–0.88 (m, C$H_{3\gamma}$ Val). FT-IR (ATR): 3298, 2964, 1631, 1528, 1440, 1232, 1153, 1044, 541 cm^{-1}.

Characterization Methods

Nuclear Magnetic Resonance Spectrometry Analysis (NMR)

NMR spectra were acquired in D$_2$O or CDCl$_3$ at 298 K on a Bruker Avance I NMR spectrometer operating at 400.2 MHz and equipped with a Bruker multinuclear z-gradient direct probe head capable of producing gradients in the z direction with 53.5 G.cm^{-1} strength. The relaxation time was fixed to 3 seconds for homonuclear correlation spectroscopy (COSY) measurements.

Mass Spectrometry Analysis (MS)

Mass spectrometry analyses were performed on a MALDI TOF/TOF (Ultraflex III, Bruker Daltonics, Bremen, Germany) equipped with a SmartBeam laser (Nd:YAG, 355 nm). Solutions of ELPs were prepared as follows: lyophilized ELPs were resuspended in water/acetonitrile (1/1, v/v) to obtain a final concentration lower than 100 μM. Samples were then mixed with the matrix solution of sinapinic acid prepared at the concentration of 10 mg/mL in water/acetonitrile (1/1, v/v). All MALDI-MS measurements were acquired in the linear positive mode and a mixture of standard proteins was used for external calibration in the suitable mass range (10−20 kDa).

Size Exclusion Chromatography (SEC)

SEC analysis was performed on a SEC-MALS system with refractive index and laser scattering detectors (WYATT Technology Optilab rEX and HELEOS-II) using an aqueous buffer (0.1 M $NaNO_3$, 0.01 M Na_2HPO_4, 0.02 M NaN_3) with a flow rate of 0.6 mL/min at 22 °C. The specific refractive index increment (dn/dc) of polysaccharide-*b*-ELP bioconjugates were measured by means of a differential refractometer (Wyatt Optilab rEX) operating at a wavelength of 658 nm at 26 °C. A single concentration of each bioconjugate was used to determine the dn/dc coefficient through the calculation module implemented in the Astra 7.1 software. The measured dn/dc values of polysaccharide-*b*-ELP bioconjugates were applied for the calculation of weight average molecular weight (M_w).

Fourier Transform Infrared Spectroscopy (FT-IR)

FT-IR spectra were recorded using a Bruker Vertex 70 spectrometer with a GladiATR diamond. Spectra were recorded directly on a powder samples at 400-4000 cm^{-1} (resolution of 4 wavenumber) range by using attenuated total reflection mode.

Transition Temperature Measurements (T_t)

T_t were determined by measuring the turbidity at 350 nm between 10 and 80 °C at a 1 °C / min^{-1} scan rate at different concentrations in DI water. Data were collected on a Cary 100 UV−Vis spectrophotometer equipped with a multicell thermoelectric temperature controller from Agilent Technologies (Les Ulis, FR). The T_t is defined as the temperature corresponding to the point where the maximum standard deviation on the absorbance versus temperature plots.

Dynamic Light Scattering Measurements (DLS)

Dynamic light scattering measurements were performed on NanoZS instrument (Malvern, U.K.) at a 90° angle at a constant position in the cuvette (constant scattering volume). The derived count rate (DCR) was defined as the mean scattered intensity normalized by the attenuation factor. The DCR was plotted against temperature and the T_t is defined as the temperature corresponding to the point where the DCR starts increasing on this plot.

Temperature-controlled Liquid Atomic Force Microscopy (Liquid AFM)

Temperature-controlled liquid atomic force microscopy measurements were performed using a Dimension FastScan Bruker AFM system. The topography images of the bioconjugates were obtained in Peak Force tapping mode, using a Silicon cantilever (ScanAsyst-Fluid+, Bruker) with a typical tip radius of 5 nm. The cantilever resonance was 150 kHz and the spring constant was 0.7 N/m. Substrates were purchased from Agar Scientific. Samples were prepared by drop-casting a bioconjugates water solution of 50 μM (150 μM for HA-*b*-ELP) onto a freshly cleaved mica or HOPG surface, which was directly applied for imaging. AFM imaging process was

conducted in liquid environment at specific temperature. An external heating stage (Bruker) was used to achieve the target temperature at the substrate surface.

RESULTS AND DISCUSSION

Synthesis of polysaccharide-*b*-ELP block copolymers

The synthetic strategy was based on a coupling reaction between the polysaccharide and ELP blocks *via* copper(I)-catalyzed azide-alkyne cycloaddition (CuAAC) which has previously been applied for biomacromolecular conjugation with high selectivity and coupling efficiency.[87] For this purpose, the three selected polysaccharides and the ELP needed to be functionalized with either an azide or an alkyne group. In most cases, polysaccharides can be straightforwardly modified at their reducing end by azide-containing amines in acidic conditions with excellent functionalization degrees. Regarding the introduction of an alkyne group at the ELP chain end, an activated alkyne-functionalized NHS-ester can be exploited and subsequently substituted by the *N*-terminal primary amine of the ELP.[84] Herein the different polysaccharides were modified at their reducing end with an azide group using a bifunctional *N*-methoxyoxyamine linker and the ELP was modified at the *N*-terminal end with an alkyne moiety (Scheme 1), allowing the subsequent coupling of the two blocks by CuAAC as illustrated on Scheme 1C.
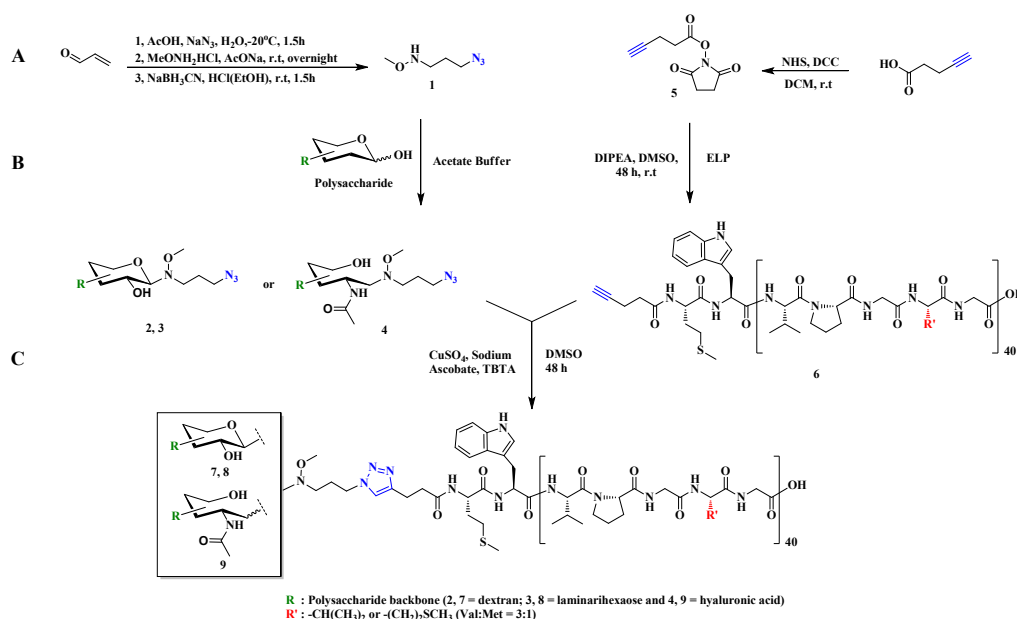
Scheme 1. Synthetic strategy of polysaccharide-*b*-elastin-like polypeptide block copolymers. (A) Synthesis of the bifunctional linker **1** and of the NHS-alkyne ester **5**. (B) Reducing-end functionalization of polysaccharides and modification of ELP at the *N*-terminus. (C) Huisgen's cycloaddition between the azide-functionalized polysaccharides and the alkyne-functionalized ELP.

Reducing-end functionalization of polysaccharides

Primary amines have been extensively used for the functionalization of polysaccharides by reductive amination to form an open-chain monosaccharide at its reducing end.[11,12] Recently the use of functional oxyamine linkers for conjugation to glycans has been demonstrated with highly efficient coupling.[82,83] In comparison to the conventional reductive amination of glycans with primary amines, the use of oxyamine linkers in acetate buffer without any reducing agent was able to produce the native closed conformation of the reducing sugar, which is essential for the recognition of some saccharides to the relevant receptors. In order to explore more on this methodology for the functionalization of polysaccharides, we first prepared the azide-functionalized oxyamine linker **1** *via* a three-step one-pot strategy (Scheme 1A) and

characterized it by 1D and 2D NMR (Figure S1).[82] This azide-linker contains an *N*-methoxyamine functional group for conjugation to the reducing end of the polysaccharides and a chain end azide group for subsequent conjugation to the ELP.[82,83] The modification reactions of Dex and Lam by the oxyamine linker were carried out in acetate buffer at 40 °C at pH 4.6 (Scheme 1B). The ^{1}H, HSQC and COSY NMR spectra in D_2O of modified polysaccharides were recorded and all peaks were assigned (see Figures S2, S3). Full conversion of Dex and Lam were confirmed by comparing the integral of the peak at 1.84 ppm corresponding to the resonance of the β-methylene of oxyamine linker with the integral of the peak at 4.1 ppm for Dex and 4.2 ppm for Lam (anomeric proton of the reducing sugar). The two protons of α-methylene in oxyamine linker have different resonance frequencies (2.89 ppm and 3.08 ppm) illustrating a stereochemical non-equivalence of the two protons, which indicated that the reducing sugar retained its closed conformation with a β-anomeric configuration due to the stereochemical effect of the methoxy group[82], and the proton coupling constant of a β-linked sugar ($J = 8.9$ Hz).

Applying the same strategy on the modification of HA by the oxyamine linker, either at pH 4.6 or 5.5 of acetate buffer gave a conversion below 50 %. This may due to the high negative charge density of HA. Thus conventional reductive amination in a buffer at pH 5.5, which has also been previously reported for the modification of HA,[11] was applied to couple the reducing end of HA with the oxyamine linker, using sodium cyanoborohydride ($NaBH_3CN$) as a reducing agent (Figure S4). Also, the integration of the NMR spectra of the starting HA and the azido-functionalized HA showed the degree of functionalization (Figure S5). As a result of the reduction, the protons of the α-methylene in the oxyamine linker have stereochemical equivalence (2.88 ppm), revealing an open chain reducing end of HA (Figure S5). Successful

azide-functionalization of the three polysaccharides was also assessed by tracking the appearance of azide vibration signal at 2100 cm^{-1} in FTIR spectra (Figure S6, S7, S8).

Alkyne functionalization at the N-terminal end of ELP

The ELP used in this work was prepared by recombinant DNA and protein engineering techniques in *Escherichia coli* as described previously.[60] This ELP contains in total 40 pentapeptide repeats with the protein sequence MW[(VPGVG)(VPGMG)(VPGVG)$_2$]$_{10}$, corresponding to a molecular weight of 17,035 Da. The ELP-polysaccharide complex reported, uses lysine-containing ELPs and charged polysaccharides as polyelectrolytes to form the complex.[78] In our strategy, we covalently conjugate the polysaccharide to the ELP to form a block copolymer, the ELP, having methionine residues, can be further functionalized to provide diverse possibilities of crosslinking or side-chain modifications.[60-62] The MS and NMR spectra characterization of this "starting" ELP are provided in Figure S9 and S10. In order to introduce an alkyne group on the ELP, the activated NHS-alkyne ester **5** was synthesized by a coupling reaction between *N*-hydroxysuccinimide and 4-pentynoic acid (Scheme 1A). The reaction of the primary amine of ELP with the NHS-alkyne ester **5** was thereafter verified by ^{1}H NMR and MALDI-Tof mass spectrometry (Figure S9, S12). Even though the terminal alkyne moiety was not detected by ^{1}H NMR spectroscopy of the purified chain end-functionalized ELP, the appearance of peaks for two methylene groups of the alkyne linker at 2.3 ppm was an indication of successful modification (Figure S12). Full alkyne functionalization of ELP was also confirmed by the MS shift to 17,119 Da after NHS-coupling chemistry (Figure S9).

Synthesis of polysaccharide-b-ELP copolymers

The emergence of "click chemistry" has revolutionized bioconjugate chemistry by affording excellent selectivity and using soft reaction conditions amenable to both synthetic polymers and

fragile biomacromolecules, such as proteins or DNAs.[88] A widely used "click reaction" is the

Cu(I)-catalyzed azide-alkyne cycloaddition or Huisgen's cycloaddition.[87] Herein, conjugations of

ELP and polysaccharides were carried out *via* Huisgen's cycloaddition in DMSO as common

solvent for the ELP and polysaccharides (Scheme 1C). TBTA, a powerful stabilizing ligand for

copper(I), was used in the conjugation of Dex and HA as they have a much higher molecular

weight than Lam. The mole ratio of polysaccharides to ELP, which are 1.5:1, 5:1 and 1:1,

for Dex, Lam and HA, respectively. The excess polysaccharides were removed by

extensive dialysis against water and the unreacted ELP was removed by inverse

transition cycling. The success of the click reaction was subsequently monitored by SEC, as

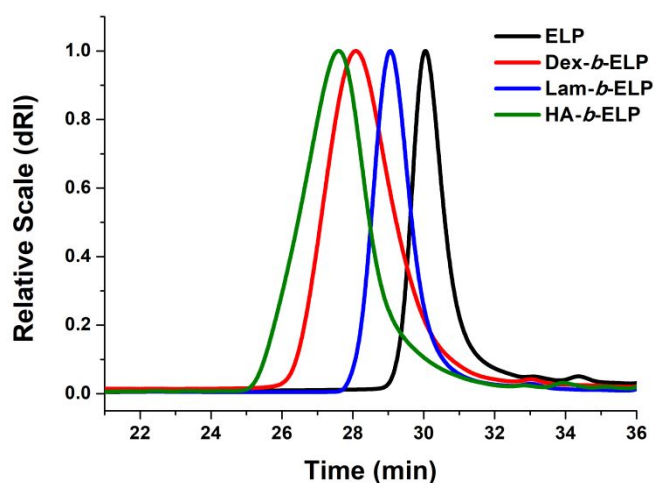well as by ^{1}H, HSQC and COSY NMR and FTIR spectroscopy.

Figure 1. SEC traces of ELP and polysaccharide-*b*-ELP bioconjugates in aqueous buffer (0.1 M

NaNO$_3$, 0.01 M Na$_2$HPO$_4$, 0.02 M NaN$_3$) using a RI detector.

The conjugation of polysaccharides to the ELP coincided with a clear increase in the molecular

weight of the different block copolymers as observed in Figure 1 and S13. SEC also highlights

the low dispersity of the resulting block copolymers (Table 1). All the peaks in ^{1}H NMR spectra were assigned with the help of corresponding HSQC and COSY NMR, indicating both polysaccharide block and ELP block (see Figure S14, S15, and S16). All NMR spectra displayed the characteristic anomeric peaks of polysaccharides at around 5.0 ppm and the triazole proton peak was found at 7.8 ppm (Figure 2) confirming the desired structures of the block copolymers. FTIR spectra of the bioconjugates, after the click reaction, were also compared with the ones of alkyne-functionalized ELP and corresponding azide-functionalized polysaccharides (Figure S6, S7 and S8). The complete disappearance of the azide band at 2100 cm^{-1} in the bioconjugates proved the success of the "click reaction" bioconjugation.

Bioconjugates	$M_w{}^{a}$ (kDa)	Polysaccharide mass fraction	PDI^{a}	T_t in water^{b} (125 μM)
Dex-*b*-ELP	24.9	32 %	1.01	39 °C
Lam-*b*-ELP	18.2	5 %	1.03	36 °C
HA-*b*-ELP	24.3	30 %	1.02	48 °C

Table 1. Characteristics of the polysaccharide-*b*-ELP bioconjugates synthesized. ^{a}Weight average molecular weight (M_w) and polydispersity index (PDI) were determined by SEC in aqueous buffer. $^{b}T_t$ was measured by turbidity on UV-Vis.
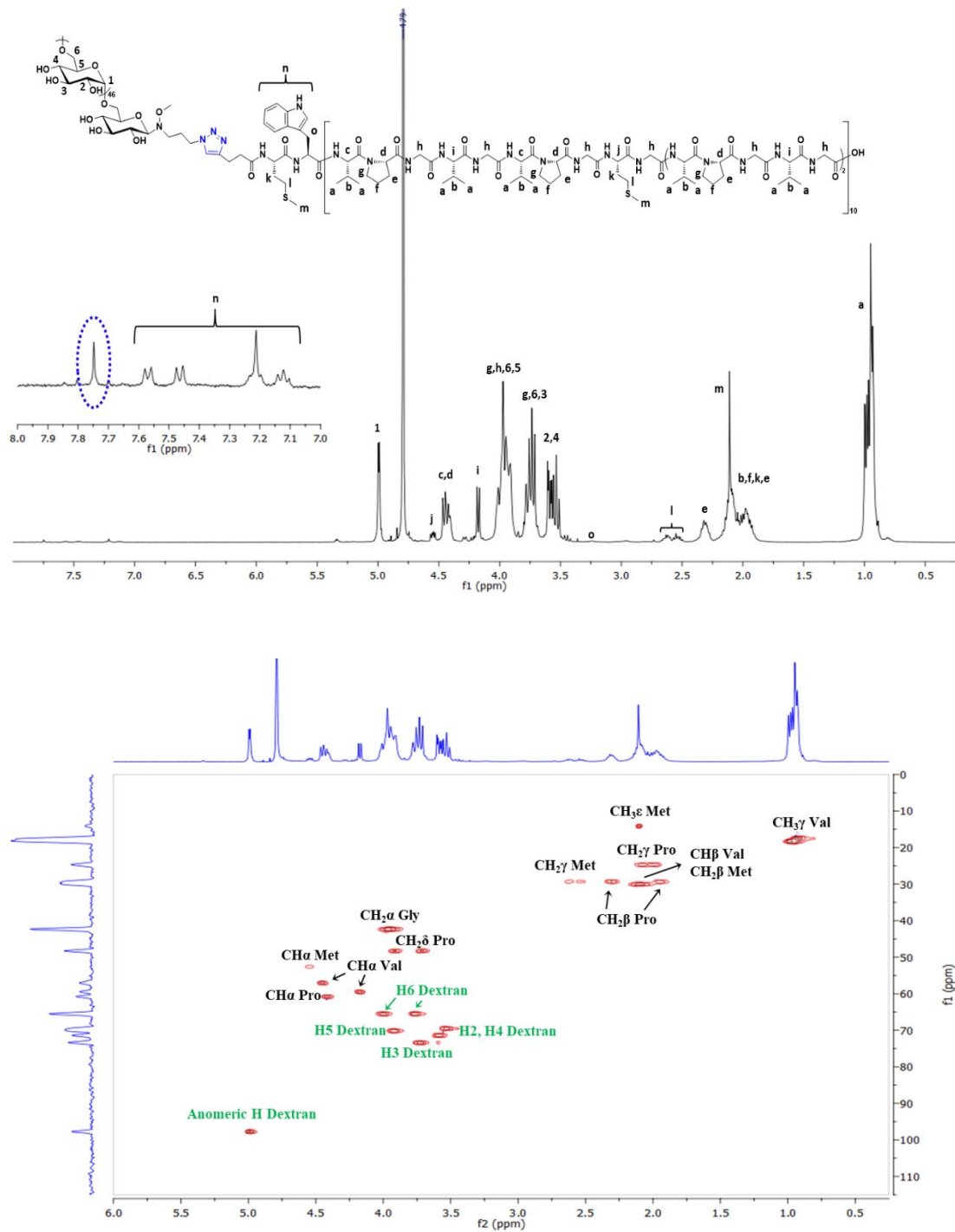
Figure 2. ^{1}H and HSQC NMR Spectra of Dex-*b*-ELP in D$_2$O at 25 °C.

Temperature-triggered self-assembly of polysaccharide-*b*-ELP copolymers

Thermo-responsive properties

The thermo-responsive properties of the different polysaccharide-*b*-ELP block copolymers were first studied by measuring the T_t values by turbidity measurement at 350 nm. In contrast with T_t of ELP (32 °C) at same concentration (Figure 3A), T_t of the bioconjugates shifted to higher temperature depending on the hydrophilicity of polysaccharides (36 °C, 39 °C and 48 °C for Lam-*b*-ELP, Dex-*b*-ELP and HA-*b*-ELP, respectively). Consistently, the higher the hydrophilicity of the polysaccharide, the larger the T_t. One can note that the slight decrease in absorption of HA-*b*-ELP at high temperature was most likely due to the formation of large aggregates, which may sediment (Figure S24). The T_t values of ELP and ELP bioconjugates were then plotted as functions of concentration (Figure 3B) and the data were fitted using the empirical law proposed by Chilkoti and coworkers.[56] This equation gave satisfactory fits of T_t, concentration and temperature, enabling accurate prediction of the T_t of ELP and its bioconjugates at specific concentrations. As the hydrophilicity of the ELP bioconjugates decreased, the slope of the fit became flatter. This result is consistent with the observations reported by Chilkoti and coworkers.[56]
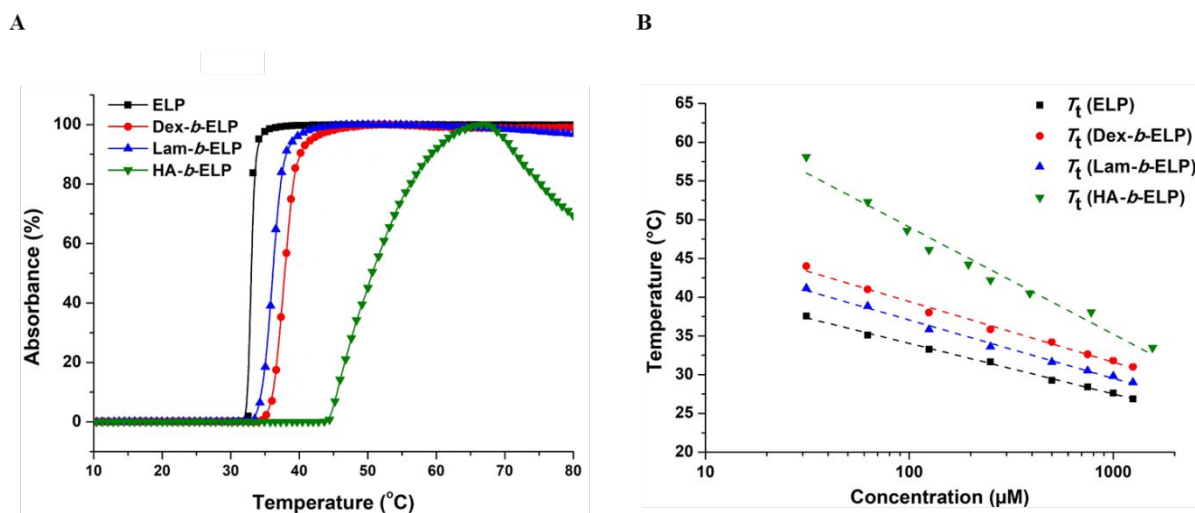
Figure 3. Turbidity study of ELP and polysaccharide-*b*-ELP bioconjugates. (A) Absorbance measured at 125 μM in water as function of temperature. (B) T_t values plotted as function of concentration in water.

Self-assembly of polysaccharide-b-ELP block copolymers

In a next step, we were interested in studying the self-assembly properties of polysaccharide-*b*-ELP copolymers and their ability to form well-defined micellar structures. The behavior of Dex-*b*-ELP (125 μM in water) was first analyzed by DLS. Measuring the total scattering intensity with temperature allowed the determination of T_t that was found to be around 40 °C. Consistently with turbidity measurements, this value was comparable and larger than the T_t of single ELP determined at the same concentration (Figure 4A) due to the conjugation of a hydrophilic polysaccharide segment. Interestingly, the physical mixture of ELP and Dex did not influence the T_t of ELP (Figure 4A, S17). As observed in Figure 4A, at low temperature (30 °C) below T_t of Dex-*b*-ELP, the scattering intensity is very low, due to the presence of free copolymer chains in solution and a few aggregates (Figure S23A). The scattering intensity sharply increased at the transition temperature (around 40 °C) and triggered the self-assembly to form structures with hydrodynamic diameter (D_h) around 165 nm. Once Dex-*b*-ELP was heated above 45 °C, the nanoparticles showed little changes in diameter with a D_h of approximately 290 nm (Figure 4B, S23A), being stable until 60 °C. Repeated heating and cooling on Dex-*b*-ELP showed similar D_h and PDI values, illustrating that this temperature-responsive behavior is fully reversible, which offers a simple method for controlling the transition of ELPs (Figure S18). Atomic force microscopy in a liquid cell was conducted to investigate the morphology of the nanostructures formed by Dex-*b*-ELP below/above T_t. Consistent with the DLS results, very small objects were observed below T_t at 35 °C (Figure 5A), and spherical-shaped particles were

observed with an average diameter of approximately 280-300 nm above T_t at 65 °C (Figure 5B)

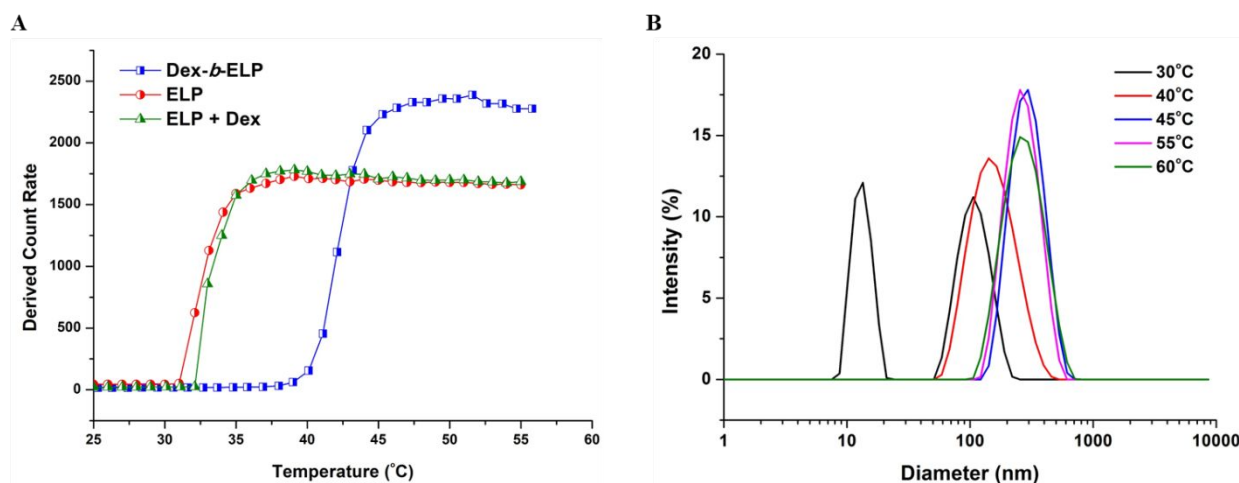and with a particle thickness around 7-10 nm (Figure S25A).

Figure 4. Dynamic light scattering analysis of the self-assembly of ELP, Dex-*b*-ELP and

physical mixture of ELP and Dex at 125 μM in water. (A) Scattered intensity as a function of

temperature upon heating. (B) Size distribution in intensity of Dex-*b*-ELP at selected

temperatures.

Due to the small hydrophilic fraction of Lam-*b*-ELP, the T_t of Lam-*b*-ELP was found around 33

°C, which is slightly higher when compared to the T_t of ELP (Figure S19). At low temperature

(30 °C), below T_t of Lam-*b*-ELP, small objects and a few aggregates were observed with very

low scattering intensity (Figure S23B). The scattering intensity sharply increased at transition

temperature (around 33 °C) and triggered the self-assembly to form structures with D_h around

210 nm (Figure S23B). Unlike Dex-*b*-ELP, a peak located at 36-38 °C was most likely due to the

formation of unstable big particles, which precipitated thus decreasing the concentration in the

detected area. Repeated heating and cooling of Lam-*b*-ELP from 25 °C to 36 °C on DLS also

illustrated this unstable behavior (Figure S20). Nevertheless the temperature-responsive behavior

of Lam-*b*-ELP is fully reversible. When temperature was heated above 45 °C, the nanoparticles

showed little changes in scattering intensity and displayed diameter with a D_h of approximately

400-500 nm (Figure S20). Liquid AFM even recorded larger diameters (500-900) for the

aggregates of Lam-*b*-ELP above the T_t (Figure 5D) and particle thickness was found around 3-5
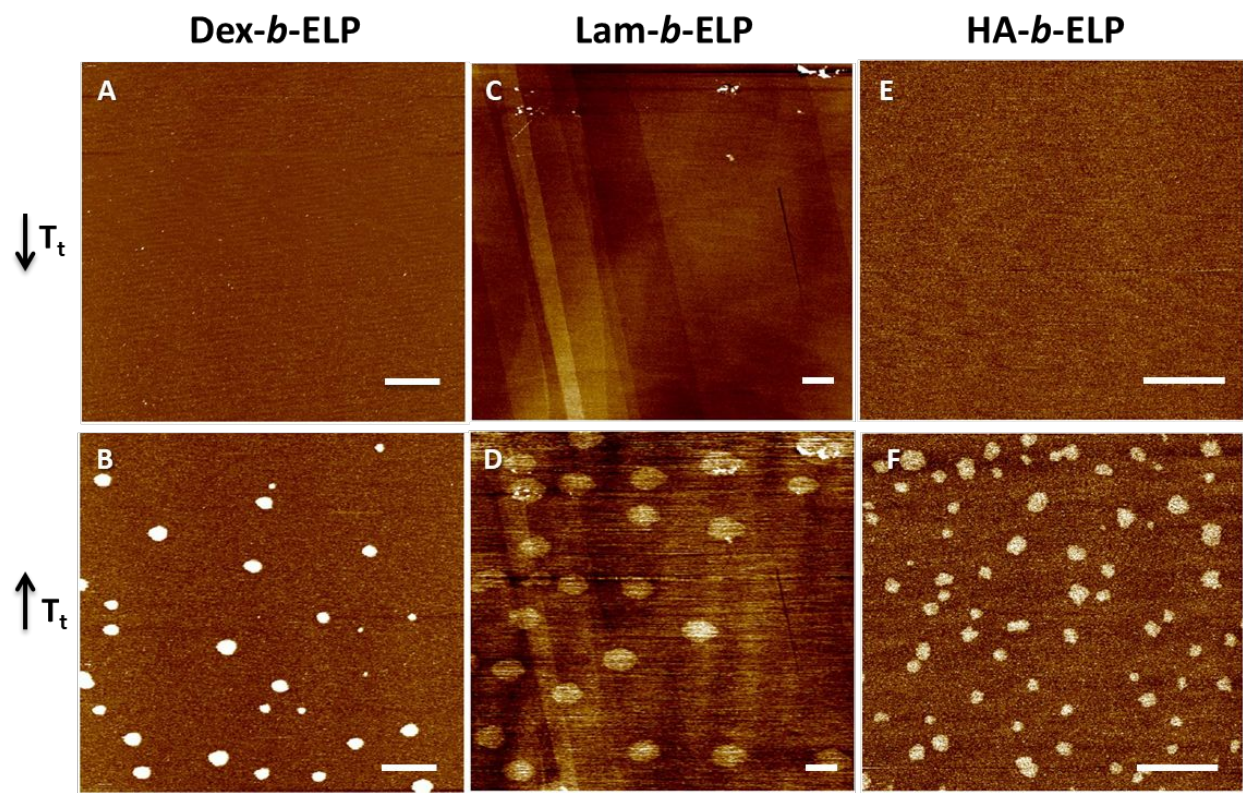
nm (Figure S25B).

Figure 5. Liquid AFM images of Dex-*b*-ELP (50 μM in water) on mica substrate at: (A) 35 °C

and (B) 65 °C. Lam-*b*-ELP (50 μM in water) on HOPG substrate at: (C) 30 °C and (D) 55 °C.

HA-*b*-ELP (150 μM in water) on mica substrate at: (E) 25 °C and (F) 52 °C. The scale bar

indicates 1 μm.

Similar to the UV-vis measurements, the T_t of HA-*b*-ELP on DLS heating ramp was found around 45 °C. At low temperature (35 °C) below T_t of HA-*b*-ELP, small objects were observed with very low scattering intensity (Figure S23C). The scattering intensity sharply increased at transition temperature and triggered the self-assembly to form structures with D_h around 300 nm at 48-50 °C (Figure S21, S23C). Once HA-*b*-ELP was heated above 55 °C, the diameter of nanoparticles became unstable and separated into two size distributions, which was also confirmed by liquid AFM (Figure S24). Nanoparticles with an average diameter of approximately 220-280 nm and a particle thickness of 0.5-1.5 nm were observed by liquid AFM at 50 °C (Figure 5F, S25C) at the same concentration. The stability of the HA-*b*-ELP assemblies at 48 °C was investigated by repeated heating and cooling on DLS. This temperature-responsive system was again found fully reversible and HA-*b*-ELP nanoparticles proved relatively stable at 48 °C for 20 minutes with an average diameter around 280 nm on every single heating time (Figure S22).

We hypothesized that the polysaccharide-*b*-ELP block copolymers may behave similarly to the ELP diblock copolymer, in which self-assembly undergoes a chain aggregation followed by ELP core dehydration[71]. However, in the presence of hydrophilic polysaccharides, molar mass and charge density of the polysaccharide, and interactions between the polysaccharide and ELP, would contribute to the "unstable" chain aggregation process. Self-assembly characteristics of polysaccharide-*b*-ELP block copolymers were summarized in Table 2.

Bioconjugates	**Conc.(µM)**	**T_t DLS**	**DLS**	**Conc.(µM)**	**AFM**

			T(°C)	Size(nm)		T(°C)	Size(nm)
Dex-*b*-ELP	125	39 °C	45	300	50	35	/
						65	190-340
Lam-*b*-ELP	125	33 °C	33	210	50	30	/
			45	520		55	500-900
HA-*b*-ELP	150	46 °C	48	300	150	25	/
						52	200-300

Table 2. Self-assembly characteristics of polysaccharide-*b*-ELP block copolymers.

CONCLUSION

We herein presented a modular approach to combine inert (Dex) and bioactive (Lam and HA) polysaccharides with a stimuli-responsive elastin-like polypeptide (ELP) into well-defined block copolymers. Polysaccharides were successfully functionalized with an azide moiety at the reducing end using a bifunctional *N*-methoxyoxyamine linker for further conjugation to the ELP. NHS-ester coupling chemistry was utilized to modify the *N*-terminal primary amine of ELP with an alkyne group. Thereafter, smart polysaccharide-*b*-ELP block copolymers were produced by CuAAC, and their thermal responsiveness was studied by turbidity measurements. Increasing temperature above the phase transition of ELP bioconjugates resulted in the formation of amphiphiles, which self-assembled into well-defined and stable nano-objects. Stable objects with a size of a few hundreds nanometers have been evidenced, especially when the hydrophilic polysaccharide segment was large enough. In addition, the self-assembly process was fully reversible by controlling the temperature. This is the first study that proposes the conjugation of bioactive polysaccharides with stimuli-responsive ELPs for the preparation of thermo-sensitive bioactive self-assemblies, providing insight into novel pathways for designing "smart" and

biologically-active nanocarriers for applications in biomaterial, drug delivery and receptor recognition.

ASSOCIATED CONTENT

Supporting Information

Synthesis route of HA-azide; Characterization (NMR, FTIR) of azide-functionalized Dex, Lam, HA and alkyne-functionalized ELP. MALDI of ELP and ELP-Alk; Characterization (SEC, NMR, FTIR) of Dex-*b*-ELP, Lam-*b*-ELP and HA-*b*-ELP. DLS heating ramp data of ELP bioconjugates; Liquid AFM images of HA-*b*-ELP at 55 °C.

AUTHOR INFORMATION

Corresponding Authors

*E-mail: garanger@enscbp.fr
*E-mail: lecommandoux@enscbp.fr

ORCID

Elisabeth Garanger: 0000-0001-9130-8286
Sébastien Lecommandoux: 0000-0003-0465-8603

Notes

The authors declare no competing financial interest.

ACKNOWLEDGEMENTS

REFERENCES

[1] Peyret, A.; Zhao, H.; Lecommandoux, S. Preparation and Properties of Asymmetric Synthetic Membranes Based on Lipid and Polymer Self-Assembly. *Langmuir* **2018**, *34* (11), 3376–3385.

[2] Trantidou, T.; Friddin, M.; Elani, Y.; Brooks, NJ.; Law, RV.; Seddon, JM.; Ces, O. Engineering Compartmentalized Biomimetic Micro- and Nanocontainers. *ACS Nano.* **2017**, *11* (7), 6549–6565.

[3] Huang, G.; Li, F.; Zhao, Xin.; Ma, Y.; Y Li.; Lin, M.; Jin, G.; Lu, TJ.; Genin, GM.; Xu, F. Functional and Biomimetic Materials for Engineering of the Three-Dimensional Cell Microenvironment. *Chem. Rev.* **2017**, *117* (20), 12764–12850.

[4] Kataoka, K.; Harada, A.; Nagasaki, Y. Block Copolymer Micelles for Drug Delivery: Design, Characterization and Biological Significance. *Adv. Drug Delivery Rev.* **2001**, *47*(1), 113–131.

[5] Eetezadi, S.; Ekdawi, SN.; Allen, C. The Challenges Facing Block Copolymer Micelles for Cancer Therapy: In Vivo Barriers and Clinical Translation. *Adv. Drug Delivery Rev.* **2015**, *91*, 7–22.

[6] Kutikov, AB.; Song, J. Biodegradable PEG-Based Amphiphilic Block Copolymers for Tissue Engineering Applications. *ACS Biomater. Sci. Eng.* **2015**, *1* (7), 463–480.

[7] Hou, Y.; Lu, H. Protein PEPylation: A New Paradigm of Protein-Polymer Conjugation. *Bioconjug. Chem.* **2019**, *30* (6), 1604–1616.

[8] Le Fer, G.; Wirotius, AL.; Brûlet, A.; Garanger, E.; Lecommandoux, S. Self-Assembly of Stimuli-Responsive Biohybrid Synthetic-*b*-Recombinant Block Copolypeptides. *Biomacromolecules* **2019**, *20* (1), 254–272.

[9] Sanson, C.; Schatz, C.; Le Meins, JF.; Brûlet, A.; Soum, A.; Lecommandoux, S. Biocompatible and Biodegradable Poly(trimethylene carbonate)-*b*-Poly(l-glutamic acid) Polymersomes: Size Control and Stability. *Langmuir* **2010**, *26* (4), 2751–2760.

[10] Zhang, A.; Zhang, Z.; Shi, F.; Xiao, C.; Ding, J.; Zhuang, X.; He, C.; Chen, L.; Chen, X. Redox-Sensitive Shell-Crosslinked Polypeptide-block-Polysaccharide Micelles for Efficient Intracellular Anticancer Drug Delivery. *Macromol. Biosci.* **2013**, *13* (9), 1249–1258.

[11] UpadHAy, KK.; Le Meins, JF.; Misra, A.; Voisin, P.; Bouchaud, V.; Ibarboure, E.; Schatz, C.; Lecommandoux, S. Biomimetic Doxorubicin Loaded Polymersomes from Hyaluronan-block-Poly(γ-benzyl glutamate) Copolymers. *Biomacromolecules* **2009**, *10* (10), 2802–2808.

[12] Schatz, C.; Louguet, S.; Le Meins, JF.; Lecommandoux. S. Polysaccharide-block-Polypeptide Copolymer Vesicles: Towards Synthetic Viral Capsids. *Angew. Chem., Int. Ed.* **2009**, *48* (14), 2572–2575.

[13] Guo, J.; Hong, H.; Chen, G.; Shi, S.; Nayak, TR.; Theuer, CP.; Barnhart, TE.; Cai, W.; Gong, S. Theranostic Unimolecular Micelles Based on Brush-Shaped Amphiphilic Block Copolymers for Tumor-Targeted Drug Delivery and Positron Emission Tomography Imaging. *ACS Appl. Mater. Interfaces.* **2014**, *6* (24), 21769–21779.

[14] Schöttner, S.; Schaffrath, HJ.; Gallei, M. Poly(2-hydroxyethyl methacrylate)-Based Amphiphilic Block Copolymers for High Water Flux Membranes and Ceramic Templates. *Macromolecules* **2016**, *49* (19), 7286–7295.

[15] Stimulus-Responsive Degradable Polylactide-Based Block Copolymer Nanoassemblies for Controlled/Enhanced Drug Delivery. *Mol. Pharm.* **2017**, *14* (8), 2460–2474.

[16] Tyler, B.; Gullotti, D.; Mangraviti, A.; Utsuki, T.; Brem, H. Polylactic acid (PLA) Controlled Delivery Carriers for Biomedical Applications. *Adv. Drug Deliv. Rev.* **2016**, *107*, 163–175.

[17] Dash, TK.; Konkimalla. VB. Polymeric Modification and Its Implication in Drug Delivery: Poly-ε-caprolactone (PCL) as a Model Polymer. *Mol. Pharm.* **2012**, *9* (9), 2365–2379.

[18] Bacinello, D.; Garanger, E.; Taton, D.; Tam, KC.; Lecommandoux, S. Enzyme-Degradable Self-Assembled Nanostructures from Polymer-Peptide Hybrids. *Biomacromolecules* **2014**, *15* (5), 1882−1888.

[19] Swierczewska, M.; Han, HS.; Kim, K.; Park, JH.; Lee, S. Polysaccharide-Based Nanoparticles for Theranostic Nanomedicine. *Adv. Drug Delivery Rev.* **2016**, *99* (Pt A), 70–84.

[20] Liu, Z.; Jiao, Y.; Wang, Y.; Zhou, C.; Zhang, Z. Polysaccharides-Based Nanoparticles as Drug Delivery Systems. *Adv. Drug Delivery Rev.* **2008**, *60* (15), 1650–1662.

[21] Rosselgong, J.; Chemin, M.; Cabral Almada, C.; Hemery, G.; Guigner, J.-M.; Chollet, Gu; Labat, G.; da Silva Perez, D.; Ham-Pichavant, F.; Grau, E.; Grelier, S.; Lecommandoux, S; Cramail, H. Synthesis and Self-Assembly of Xylan-Based Amphiphiles: From Bio-Based Vesicles to Antifungal Properties. *Biomacromolecules* **2019**, *20* (1), 118–129.

[22] Rabotyagova, OS.; Cebe, P.; Kaplan, DL. Protein-Based Block Copolymers. *Biomacromolecules* **2011**, *12* (2), 269–289.

[23] Seidi, K.; Neubauer, HA.; Moriggl, R.; Jahanban-Esfahlan, R.; Javaheri, T. Tumor Target Amplification: Implications for Nano Drug Delivery Systems. *J. Controlled Release* **2018**, *275*, 142–161.

[24] Cai, L.; Gu, Z.; Zhong, J.; Wen, D.; Chen, G.; He, L.; Wu, J.; Gu, Z. Advances in Glycosylation-Mediated Cancer-Targeted Drug Delivery. *Drug Discov. Today* **2018**, *23* (5), 1126–1138.

[25] Huang, GL.; Huang, HL. Hyaluronic Acid-based Biopharmaceutical Delivery and Tumor-Targeted Drug Delivery System. *J. Controlled Release* **2018**, *278*, 122–126.

[26] Wang, SS.-S.; How, S-C.; Chen, Y-D.; Tsaic, Y-H.; Jan J-S. Bioactive Saccharide-Conjugated Polypeptide Micelles for Acid-Triggered Doxorubicin Delivery. *J. Mater. Chem. B*, **2015**, *3*, 5220–5231.

[27] Huang, J.; Bonduelle, C.; Thévenot, J.; Lecommandoux, S.; Heise, A. Biologically Active Polymersomes from Amphiphilic Glycopeptides. *J. Am. Chem. Soc.* **2012**, *134* (1), 119−122.

[28] Garanger, E.; Lecommandoux, S. Towards Bioactive Nanovehicles Based on Protein Polymers. *Angew. Chem., Int. Ed.* **2012**, *51* (13), 3060–3062.

[29] Bonduelle, C.; Lecommandoux, S. Synthetic Glycopolypeptides as Biomimetic Analogues of Natural Glycoproteins. *Biomacromolecules* **2013**, *14* (9), 2973–2983.

[30] Ahsan, SM.; Thomas, M.; Reddy, KK.; Sooraparaju, SG.; Asthana, A.; Bhatnagar, I. Chitosan as biomaterial in drug delivery and tissue engineering. *Int. J. Biol. Macromol.* **2018**, *110*, 97−109.

[31] VK Thakur.; MK Thakur. Recent Advances in Graft Copolymerization and Applications of Chitosan: A Review. *ACS Sustainable Chem. Eng.* **2014**, *212*, 2637–2652.

[32] Gu, D.; Huang, L.; Chen, X.; Wu, Q.; Ding, K. Structural Characterization of a Galactan From Ophiopogon Japonicus and Anti-Pancreatic Cancer Activity of Its Acetylated Derivative. *Int. J. Biol. Macromol.* **2018**, *113*, 907–915.

[33] Chiang, CS.; Lin, YJ.; Lee, R.; Lai, YH.; Cheng, HW.; Hsieh, CH.; Shyu, WC.; Chen, SY. Combination of Fucoidan-Based Magnetic Nanoparticles and Immunomodulators Enhances Tumour-Localized Immunotherapy. *Nat. Nanotechnol.* **2018**, *13* (8), 746–754.

[34] Duan, H.; Donovan, M.; Foucher, A.; Schultze, X.; Lecommandoux, S. Multivalent and Multifunctional Polysaccharide-Based Particles for Controlled Receptor Recognition. *Sci. Rep.* **2018**, *8* (1), 14730.

[35] Schatz, C.; Lecommandoux, S. Polysaccharide-Containing Block Copolymers: Synthesis, Properties and Applications of an Emerging Family of Glycoconjugates. *Macromol. Rapid Commun.* **2010**, *31*(19), 1664–1684.

[36] Hu, X.; Zhang, Y.; Xie, Z.; Jing, X.; Bellotti, A.; Gu, Z. Stimuli-Responsive Polymersomes for Biomedical Applications. *Biomacromolecules* **2017**, *18* (3), 649–673.

[37] Cobo, I.; Li, M.; Sumerlin, BS.; Perrier, S. Smart Hybrid Materials by Conjugation of Responsive Polymers to Biomacromolecules. *Nat. Mater.* **2015**, *14* (2), 143–159.

[38] Stuart, M. A. C.; Huck, W. T.; Genzer, J.; Müller, M.; Ober, C.; Stamm, M.; Sukhorukov, G. B.; Szleifer, I.; Tsukruk, V. V.; Urban, M. Emerging Applications of Stimuli-Responsive Polymer Materials. *Nat. Mater.* **2010**, *9* (2), 101–113.

[39] Hoffman, AS. Stimuli-Responsive Polymers: Biomedical Applications and Challenges for Clinical Translation. *Adv. Drug Deliv. Rev.* **2013**, *65* (1), 10–16.

[40] Bajpai, A.K.; Shukla, SK.; Bhanu, S.; Kankane, S. Responsive Polymers in Controlled Drug Delivery. *Prog. Polym. Sci.* **2008**, *33* (11), 1088–1118.

[41] Roy, D.; Cambre, JN.; Sumerlin, BS. Future Perspectives and Recent Advances in Stimuli-Responsive Materials. *Prog. Polym. Sci.* **2010**, *35* (1-2), 278–301.

[42] Pang, X.; Jiang, Y.; Xiao, Q.; Leung, AW.; Hua, H.; Xu, C. pH-responsive polymer-drug conjugates: Design and progress. *J. Controlled Release.* **2016**, *222*, 116–129.

[43] Peeler, DJ.; Sellers, DL.; Pun, SH. pH-Sensitive Polymers as Dynamic Mediators of Barriers to Nucleic Acid Delivery. *Bioconjugate Chem.* **2019**, *30* (2), 350–365.

[44] Sun, H.; Zhang, Y.; Zhong, Z. Reduction-Sensitive Polymeric Nanomedicines: An Emerging Multifunctional Platform for Targeted Cancer Therapy. *Adv. Drug Deliv. Rev.* **2018**, *132*, 16–32.

[45] An, X.; Zhu, A.; Luo, H.; Ke, H.; Chen, H.; Zhao, Y. Rational Design of Multi-Stimuli-Responsive Nanoparticles for Precise Cancer Therapy. *ACS Nano.* **2016**, *10* (6), 5947–5958.

[46] Anderson, C. F.; Cui, H. Protease-Sensitive Nanomaterials for Cancer Therapeutics and Imaging. *Ind Eng Chem Res*. **2017**, *56* (20), 5761–5777.

[47] Kim, W.; Thévenot, J.; Ibarboure, E.; Lecommandoux, S.; Chaikof, E. L. Self-Assembly of Thermally Responsive Amphiphilic Diblock Copolypeptides into Spherical Micellar Nanoparticles. *Angew. Chem., Int. Ed.* **2010**, *122* (25), 4353– 4356.

[48] Strandman, S.; Zhu, X.X. Thermo-Responsive block Copolymers with Multiple Phase Transition Temperatures in Aqueous Solutions. *Prog. Polym. Sci.* **2015**, *42*, 154–176.

[49] Beauté, L.; McClenaghan, N.; Lecommandoux, S. Photo-Triggered Polymer Nanomedicines: From Molecular Mechanisms to Therapeutic Applications. *Adv. Drug Deliv. Rev.* **2019**, *138*, 148–166.

[50] Zhao, Y. Light-Responsive Block Copolymer Micelles. *Macromolecules* **2012**, *45* (9), 3647–3657.

[51] Reddy, LH.; Arias, JL.; Nicolas, J.; Couvreur, P. Targeted Drug Delivery with Polymers and Magnetic Nanoparticles: Covalent and Noncovalent Approaches, Release Control, and Clinical Studies. *Chem. Rev.* **2012**, *112* (11), 5818–5878.

[52] MacEwan, S. R.; Chilkoti, A. Applications of Elastin-like Polypeptides in Drug Delivery. *J. Controlled Release* **2014**, *190*, 314–330.

[53] McDaniel, J. R.; Callahan, D. J.; Chilkoti, A. Drug Delivery to Solid Tumors by Elastin-Like Polypeptides. *Adv. Drug Delivery Rev.* **2010**, *62* (15), 1456–1467.

[54] Despanie, J.; Dhandhukia, JP.; Hamm-Alvarez, SF.; MacKay, JA. Elastin-Like Polypeptides: Therapeutic Applications for an Emerging Class of Nanomedicines. *J. Controlled Release* **2016**, *240*, 93–108.

[55] Halperin, A.; Kröger, M.; Winnik, FM. Poly(N-isopropylacrylamide) Phase Diagrams: Fifty Years of Research. *Angew. Chem., Int. Ed*. **2015**, *54* (51), 15342–15367.

[56] Meyer, D. E.; Chilkoti, A. Quantification of the Effects of Chain Length and Concentration on the Thermal Behavior of Elastin-like Polypeptides. *Biomacromolecules* **2004**, *5* (3), 846−851.

[57] Li, N. K.; Roberts, S.; Quiroz, F. G.; Chilkoti, A.; Yingling, Y. G. Sequence Directionality Dramatically Affects LCST Behavior of Elastin-Like Polypeptides. *Biomacromolecules* **2018**, *19* (7), 2496–2505.

[58] MacEwan, S. R.; Weitzhandler, I.; Hoffmann, I.; Genzer, J.; Gradzielski, M.; Chilkoti, A. Phase Behavior and Self-Assembly of Perfectly Sequence-Defined and Monodisperse Multiblock Copolypeptides. *Biomacromolecules* **2017**, *18* (2), 599–609.

[59] van Eldijk, MB.; Smits, FC.; Vermue, N.; Debets, MF.; Schoffelen, S.; van Hest, JC. Synthesis and Self-Assembly of Well-Defined Elastin-Like Polypeptide-Poly (ethylene glycol) Conjugates. *Biomacromolecules* **2014**, *15* (7), 2751–2759.

[60] Petitdemange, R.; Garanger, E.; Bataille, L.; Dieryck, W.; Bathany, K.; Garbay, B.; Deming, TJ.; Lecommandoux, S. Selective Tuning of Elastin-like Polypeptide Properties via Methionine Oxidation. *Biomacromolecules* **2017**, *18* (2), 544–550.

[61] Petitdemange, R.; Garanger, E.; Bataille, L.; Bathany, K.; Garbay, B.; Deming, TJ.; Lecommandoux, S. Tuning Thermoresponsive Properties of Cationic Elastin-like Polypeptides by Varying Counterions and Side-Chains. *Bioconjugate Chem.* **2017**, *28* (5), 1403–1412.

[62] Kramer, J. R.; Petitdemange, R.; Bataille, L.; Bathany, K.; Wirotius, A.-L.; Garbay, B.; Deming, T. J.; Garanger, E.; Lecommandoux, S. Quantitative Side-Chain Modifications of Methionine-Containing Elastin-Like Polypeptides as a Versatile Tool to Tune Their Properties. *ACS Macro. Lett.* **2015**, *4* (11), 1283–1286.

[63] Malho, JM.; Brand, J.; Pecastaings, G.; Ruokolainen, J.; Gröschel, A.; Sèbe, G.; Garanger, E.; Lecommandoux, S. Multifunctional Stimuli-Responsive Cellulose Nanocrystals via Dual Surface Modification with Genetically Engineered Elastin-Like Polypeptides and Poly(acrylic acid). *ACS Macro. Lett.* **2018**, *7* (6), 646–650.

[64] Ott, W.; Nicolaus, T.; Gaub, HE.; Nash, MA. Sequence-Independent Cloning and Post-Translational Modification of Repetitive Protein Polymers through Sortase and Sfp-Mediated Enzymatic Ligation. *Biomacromolecules* **2016**, *17* (4), 1330–1338.

[65] Seifried, BM.; Cao, J.; Olsen, BD. Multifunctional, High Molecular Weight, Post-Translationally Modified Proteins through Oxidative Cysteine Coupling and Tyrosine Modification. *Bioconjugate Chem.* **2018**, *29* (6), 1876-1884.

[66] Zhu, D.; Wang, H.; Trinh, P.; Heilshorn, SC. Yang F. Elastin-like Protein-Hyaluronic Acid (ELP-HA) Hydrogels with Decoupled Mechanical and Biochemical Cues for Cartilage Regeneration. *Biomaterials* **2017**, *127*, 132–140.

[67] Dreher, M. R.; Raucher, D.; Balu, N.; Colvin, O. M.; Ludeman, S. M.; Chilkoti, A. Evaluation of an Elastin-Like Polypeptide–Doxorubicin Conjugate for Cancer Therapy. *J. Controlled Release* **2003**, *91* (1-2), 31–43.

[68] Wang, Z.; He, Q.; Zhao, W.; Luo, J.; Gao, W. Tumor-homing, pH- and Ultrasound-Responsive Polypeptide-Doxorubicin Nanoconjugates Overcome Doxorubicin Resistance in Cancer Therapy. *J. Controlled Release* **2017**, *264*, 66–75.

[69] Dreher, M. R.; Simnick, A. J.; Fischer, K.; Smith, R. J.; Patel, A.; Schmidt, M.; Chilkoti, A. Temperature Triggered Self-Assembly of Polypeptides into Multivalent Spherical Micelles. *J. Am. Chem. Soc.* **2008**, *130* (2), 687–694.

[70] Hassouneh, W.; Zhulina, E. B.; Chilkoti, A.; Rubinstein, M. Elastin-Like Polypeptide Diblock Copolymers Self-Assemble into Weak Micelles. *Macromolecules* **2015**, *48* (12), 4183–4195.

[71] Garanger, E.; MacEwan, S. R.; Sandre, O.; Brûlet, A.; Bataille, L.; Chilkoti, A.; Lecommandoux, S. Structural Evolution of a Stimulus-Responsive Diblock Polypeptide Micelle by Temperature Tunable Compaction of its Core. *Macromolecules* **2015**, *48* (18), 6617–6627.

[72] Hassouneh W1, Fischer K, MacEwan SR, Branscheid R, Fu CL, Liu R, Schmidt M, Chilkoti A. Unexpected Multivalent Display of Proteins by Temperature Triggered Self-Assembly of Elastin-like Polypeptide Block Copolymers. *Biomacromolecules* **2012**, *13* (5), 1598-1605.

[73] Pille, J.; van Lith, SA.; van Hest, JC.; Leenders, WP. Self-Assembling VHH-Elastin-Like Peptides for Photodynamic Nanomedicine. *Biomacromolecules* **2017**, *18* (4), 1302–1310.

[74] Chen, TH.; Bae, Y.; Furgeson, DY. Intelligent Biosynthetic Nanobiomaterials (IBNs) for Hyperthermic Gene Delivery. *Pharm. Res.* **2008**, *25* (3), 683–691.

[75] Le Fer, G.; Portes, D.; Goudounet, G.; Guigner, J.-M.; Garanger, E.; Lecommandoux, S. Design and Self-Assembly of PBLG-b-ELP Hybrid Diblock Copolymers Based on Synthetic and Elastin-Like Polypeptides. *Org. Biomol. Chem.* **2017**, *15* (47), 10095–10104.

[76] Fujita, Y.; Mie, M.; Kobatake, E. Construction of Nanoscale Protein Particle Using Temperature-Sensitive Elastin-like Peptide and Polyaspartic Acid Chain. *Biomaterials* **2009**, *30* (20), 3450–3457.

[77] Araújo, A.; Olsen, BD.; Machado, AV. Engineering Elastin-Like Polypeptide-Poly (ethylene glycol) Multiblock Physical Networks. *Biomacromolecules* **2018**, *19* (2), 329–339.

[78] Tang, JD.; Caliari, SR.; Lampe, KJ. Temperature-Dependent Complex Coacervation of Engineered Elastin-like Polypeptide and Hyaluronic Acid Polyelectrolytes. *Biomacromolecules* **2018**, *19* (10), 3925–3935.

[79] Jeannot, V.; Gauche, C.; Mazzaferro, S.; Couvet, M.; Vanwonterghem, L.; Henry, M.; Didier, C.; Vollaire, J.; Josserand, V.; Coll, JL.; Schatz, C.; Lecommandoux, S.; Hurbin, A. Anti-Tumor Efficacy of Hyaluronan-based Nanoparticles for the Co-Delivery of Drugs in Lung Cancer. *J. Controlled Release* **2018**, *275*, 117–128.

[80] Jeannot, V.; Mazzaferro, S.; Lavaud, J.; Vanwonterghem, L.; Henry, M.; Arboléas, M.; Vollaire, J.; Josserand, V.; Coll, JL.; Lecommandoux, S.; Schatz, C.; Hurbin, A. Targeting CD44 Receptor-Positive Lung Tumors Using Polysaccharide-Based Nanocarriers: Influence of Nanoparticle Size and Administration Route. *Nanomedicine* **2016**, *12* (4), 921–932.

[81] Pickens, CJ.; Johnson, SN.; Pressnall, MM.; Leon, MA.; Berkland, CJ. Practical Considerations, Challenges, and Limitations of Bioconjugation via Azide-Alkyne Cycloaddition. *Bioconjugate Chem.* **2018**, *29* (3), 686−701.

[82] Munneke, S.; Prevost, JR.; Painter, GF.; Stocker, BL.; Timmer, MS. The Rapid and Facile Synthesis of Oxyamine Linkers for the Preparation of Hydrolytically Stable Glycoconjugates. *Org. Lett.* **2015**, *17* (3), 624–627.

[83] Munneke, S.; Hill, JC.; Timmer, MS.; Stocker, BL.; Synthesis and Hydrolytic Stability of N- and O-Methyloxyamine Linkers for the Synthesis of Glycoconjugates. *Eur. J. Org. Chem.* **2017**, *25*, 3722–3728.

[84] Ward, CC. ; Kleinman, JI. ; Nomura, DK. NHS-Esters as Versatile Reactivity-Based

Probes for Mapping Proteome-Wide Ligandable Hotspots. *ACS Chem. Biol.* **2017**, *12* (6),

1478–1483.

[85] Tanaka, H,; Kawai, T.; Adachi, Y.; Ohno, N.; Takahashi, T. β(1,3) Branched Heptadeca-

and Linear Hexadeca-Saccharides Possessing an Aminoalkyl Group as a Strong Ligand to

Dectin-1. *Chem. Commun.* **2010**, *46* (43), 8249–8251.

[86] Palma, AS.; Feizi, T.; Zhang, Y.; Stoll, MS.; Lawson, AM.; Díaz-Rodríguez, E.;

Campanero-Rhodes, MA.; Costa, J.; Gordon, S.; Brown, GD.; Chai, W. Ligands for the β-

Glucan Receptor, Dectin-1, Assigned Using "Designer" Microarrays of Oligosaccharide

Probes (Neoglycolipids) Generated from Glucan Polysaccharides. *J. Biol. Chem.* **2006**, *281*

(9), 5771–5779.

[87] Tiwari, VK.; Mishra, BB1.; Mishra, KB.; Mishra, N.; Singh, AS.; Chen, X. Cu-Catalyzed

Click Reaction in Carbohydrate Chemistry. *Chem. Rev.* **2016**, *116* (5), 3086–3240.

[88] Thirumurugan, P.; Matosiuk, D.; Jozwiak, K. Click Chemistry for Drug Development and

Diverse Chemical–Biology Applications. *Chem. Rev.* **2013**, *113* (7), 4905–4979.